Refueling Tokamaks by Injection of Compact Toroids

P. B. Parks
General Atomics, San Diego, California 92138-5608
(Received 22 December 1987)

It is shown that transverse injection of a hypervelocity high-density spheromak plasmoid into a tokamak plasma may be a viable fueling scheme. Three important processes occur and are discussed individually: establishment of equilibrium, slowing down, and disassembly of the compact toroid.

PACS numbers: 52.55.Fa, 52.55.Hc

Several advantages are gained by fueling directly in the core of a fusioning tokamak plasma, varying from more efficient utilization of DT fuel to improvement in the energy confinement time.[1-4] The conventional method of fueling by pellet injection may not be adequate for large hot fusion-grade plasmas because of the demanding technological requirements needed to accelerate pellets to the necessary high velocities $\gtrsim 10$ km/s. However, compact toroid (CT) plasmoids have been produced and routinely accelerated to velocities of $>10^3$ km/s in the RACE coaxial gun experiments of Hammer, Hartman, and Eddeman.[5] By virtue of their high velocities, fueling tokamak plasmas by hypervelocity plasmoid injection has recently been proposed by Perkins, Ho, and Hammer as a candidate fueling scheme for the experimental test reactor (ETR).[6]

This Letter describes a model for the interaction between a moving CT plasmoid and a magnetized plasma in relation to the feasibility of the scheme. We first examine how the moving CT is held fixed in equilibrium by the background tokamak magnetic field, which is diamagnetically excluded from the interior of the CT. We then estimate its deceleration time and the time to decay by surface and volume resistive dissipation processes. We specialize to the case of a spherically shaped CT without the hole, i.e., a spheromak.[7,8] For definiteness we choose ETR parameters. The CT mass for a $\sim 10\%$ density perturbation (1-Hz rate coaxial injector) is around $M_1 \sim 4.5$ mg.[6] Bearing in mind that the CT must be small enough to pass through a wall aperture, we choose a radius $r_1 \sim 10$ cm, giving an average CT ion density of $n_1 \sim 2\times 10^{17}$ cm^{-3}.

We assume that the CT is injected with velocity $V_{\rm inj}\hat{\mathbf{x}}$ perpendicular to the undisturbed background magnetic field $B_\infty \hat{\mathbf{z}}$. After the CT exits the gun, it is for an instant deconfined. Its poloidal magnetic field will then appear to have a dipole character, with dipole moment $\mathbf{m} \sim \pi I_t r_1^2/c\hat{\mathbf{x}}$ originally oriented perpendicular to the background magnetic field, where I_t is the toroidal current inside the CT. As soon as the CT enters the vacuum tokamak magnetic field region, it will begin to rotate under torque $\mathbf{m}\times\mathbf{B}_\infty$ until the magnetic moment and $\mathbf{B}_\infty$ are aligned parallel to each other. The characteristic time constant for this being $\tau_{\rm tilt} \sim (mB_\infty/I_m)^{1/2}$ in which $I_m = \frac{5}{2} M_1 r_1^2$ is the appropriate moment of inertia. The characteristic magnetic field inside the CT, B_1, must be comparable to B_∞ in order that the closed magnetic field line topology remain intact. Since $I_t \propto r_1 B_1$, the "tilt time" can be expressed as $t_{\rm tilt} \sim \tau_{\rm A1} \equiv r_1/V_{\rm A1}$ where $V_{\rm A1} = B_\infty/(4\pi n_1 m_i)^{1/2}$ is the Alfvén speed in the CT. Taking the above parameters with $B_\infty = 50$ kG gives $V_{\rm A1} = 154$ km/s and $t_{\rm tilt} = 0.65$ μs. This will be seen to be the shortest time scale of interest here so that the realignment of the CT with its axis of rotation parallel to the background magnetic field occurs almost immediately after its encounter with this field. Numerical magnetohydrodynamics (MHD) simulations also show that the CT tilts 90° in about an Alfvén time, $\tau_{\rm A1}$.[9]

In the following, we demonstrate how the CT, once embedded inside the tokamak magnetic field, may propagate across the field without expanding and stopping prematurely. We consider the mode of propagation in which the injected kinetic energy density at injection exceeds the background magnetic field energy density $\frac{1}{2} m_i n_1 V_{\rm inj}^2 > B_\infty^2/8\pi$. This assures penetration of the CT through the background magnetic field which will be excluded from the interior of the CT and slip around its periphery. Since the injection energy goes into translational kinetic energy and the energy needed to exclude the magnetic field, the CT begins to move through the field with initial velocity

$$V_{\rm CT0} = (V_{\rm inj}^2 - V_{\rm A1}^2)^{1/2}. \tag{1}$$

As shown in Fig. 1, the final configuration is such that no external magnetic flux links the CT region making it possible for it to easily penetrate the tokamak plasma region without stretching or breaking field lines. A spheroidal current sheet appears at the boundary separating oppositely directed tangential magnetic fields on each side of it (Fig. 1). Since the speed of the CT is such that $V_{\rm CT} \ll V_{\rm A0}$ where $V_{\rm A0} = (B_\infty^2/4\pi m_i n_0)$ is the Alfvén speed of the background plasma of density n_0, the deformed background tokamak magnetic field B_0 will respond quickly by setting up a series of quasiequilibria characterized by vanishing current density, $\nabla\times\mathbf{B}_0 \cong 0$, to lowest order in $V_{\rm CT}^2/V_{\rm A0}^2$. In a polar coordinate system (r,θ,ϕ) with the polar axis pointing in the z direction and origin at the center of the sphere, the resulting external

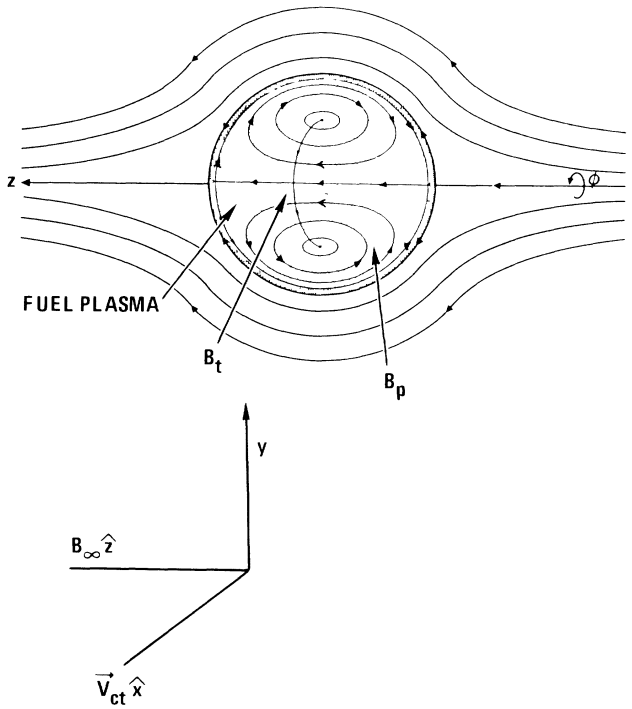

FIG. 1. Magnetic field topology in the vicinity of a compact spheromak moving in $+\hat{\mathbf{x}}$ direction. A spheroid current sheet (shaded circle) separates oppositely directed magnetic field lines.

field components are $B_{0r}=-B_\infty(1-r_1^3/r^3)\cos\theta$, $B_{0\theta}=-\frac{1}{2}B_\infty(2+r_1^3/r^3)\sin\theta$, where B_∞ is the assumed uniform tokamak magnetic field asymptotically far from the CT. At the current sheet $r=r_1$ the external tangential magnetic field is $B_{0\theta}(r=r_1)=-\frac{3}{2}B_\infty\sin\theta$.

In the interior CT region, the magnetic field B_1 is assumed to have the force-free Taylor configuration $\nabla\times\mathbf{B}_1=\mu\mathbf{B}_1$, with the current density being $\mathbf{J}_1=\mu\mathbf{B}_1/\mu_0$. The classical spheromak solutions for a vanishing radial component on a conducting wall placed at $r=r_1$ are[7]

$$B_{1r}=2C\cos\theta j_1(x)/x,$$
$$B_{1\theta}=-C\sin\theta x^{-1}d(xj_1)/dx, \tag{2}$$
$$B_{1\phi}=C\sin\theta j_1(x),$$

where $x=\mu r$ and $\mu r_1=4.493$ is the first zero of the spherical Bessel function of order 1. In this problem the current sheet replaces the perfectly conducting wall. Since the oppositely directed tangential magnetic field components on each side of the current sheet have the same $\sin\theta$ dependence they can be made equal in magnitude $|B_{1\theta}|=|B_{0\theta}|$ over the entire surface by letting $C=6.904B_\infty$. With this normalization, the toroidal and poloidal currents inside the spheromak are, respectively, $I_t(A)=6.43\times10^6 r_1(m)B_\infty(T)$, and $I_p(A)=8.036\times10^6 r_1(m)B_\infty(T)$.

Thus, once the CT is embedded in the external magnetic field, pressure equilibrium across the current sheet should be assured, i.e., $B_{1\theta}^2=B_{0\theta}^2$, and expansion of the CT should be prevented. The essential differences between CT plasmoid injection and injection of a bare plasmoid ball without embedded magnetic fields is that the outward pressure inside the ball being isotropic cannot balance the anisotropic external magnetic field pressure exerted on its surface. Inevitably, the bare plasmoid will expand axially at the Alfvén speed V_{A1} lowering its density to the point where it can no longer propagate.

To estimate the amount of drag due to Alfvén wave emission, we start by considering the magnitude of the electric fields and plasma flows induced by the motion of the CT across the magnetic field. We first look at the problem in the comoving frame of reference, f', which is instantaneously moving with velocity $\mathbf{V}_{CT}=V_{CT}\hat{\mathbf{x}}$ relative to frame f, which contains an observer at rest. The field variables as seen in f' are related to those seen in f by $\mathbf{E}'=\mathbf{E}+(\mathbf{V}_{CT}\times\mathbf{B})/c$, $\mathbf{B}'=\mathbf{B}$, $\rho_c'=\rho_c-(1/c^2)\mathbf{V}_{CT}\cdot\mathbf{J}$, and $\mathbf{J}'=\mathbf{J}-\rho_c\mathbf{V}_{CT}$.

Far from the CT $E\to0$, $\mathbf{B}\to\mathbf{B}_\infty$ so that in the comoving frame f' the CT appears to be immersed in a uniform background electric field in the $-y$ direction:

$$\mathbf{E}_\infty'=-V_{CT}B_\infty\hat{\mathbf{y}}/c. \tag{3}$$

Since the CT may be regarded as a good conductor, it excludes all external fields; i.e., inside the CT $\mathbf{B}'=\mathbf{B}_1$ and $\mathbf{E}'=0$. In the region outside the CT there is no electric field along the magnetic field lines because of the high background plasma conductivity parallel to the field lines. All field variables are time stationary in f' so that we can write $\mathbf{E}'=-\nabla\Phi$. It is convenient to express the electric potential Φ in terms of the two independent variables ψ and ϕ since $\Phi(\psi,\phi)$ automatically satisfies the condition $\mathbf{E}'\cdot\mathbf{B}_0'=0$. Polarization surface charges develop on the surface of the CT in order to have zero electric field inside and a volume charge density ρ_c' develops in the background plasma to cancel out parallel electric fields induced by these surface charges. Since charges cannot move across magnetic flux surfaces, the charges within a flux tube become reshuffled keeping the total net charge zero, i.e.,

$$\int_{-\infty}^{+\infty}\frac{dl}{B_0'}\rho_c'=0, \tag{4}$$

where the integral over dl is a line integral along $\mathbf{B}_0'$. This constraint together with the Maxwell equation $\rho_c'=(\nabla\cdot\mathbf{E}')/4\pi$ allows us to construct a partial differential equation for the potential $\Phi(\psi,\phi)$

$$\frac{\partial^2\Phi}{\partial\psi^2}+\frac{\partial\Phi}{\partial\psi}W(\psi)+U(\psi)\frac{\partial^2\Phi}{\partial\phi^2}=0, \tag{5}$$

where we have introduced the following designations:

$$W(\psi)=Q(\psi)/P(\psi),\quad U(\psi)=R(\psi)/P(\psi),$$
$$P(\psi)=\langle|\nabla\psi|^2\rangle,\quad Q(\psi)=\langle\nabla^2\psi\rangle, \tag{6}$$
$$R(\psi)=\langle(r^2\sin\theta)^{-1}\rangle,$$

and the angle brackets stand for $\int_{-\infty}^{+\infty} \ldots dl/B_0'$.

We next expand $\Phi(\psi,\phi)$ in the form

$$\Phi(\psi,\phi)=\sum_{m=1}^{\infty} H_m(\psi)\sin m\phi, \tag{7}$$

and substitute into Eq. (5) to obtain a differential equation for the individual H_m's. With the transformation $H_m(\psi)=G_m(\psi)\exp-\frac{1}{2}\int W\,d\psi$ this is

$$d^2G_m/d\psi^2-(\tfrac{1}{2}\,dW/d\psi+\tfrac{1}{4}W^2-m^2U)G_m=0. \tag{8}$$

Because of the extremely complex nature of the W,U functions, a complete solution of Eq. (8) is evidently difficult. Asymptotic solutions of Eq. (8) far from the CT can be found by taking the limiting forms of W and U for large ψ, i.e., $W(\psi)\rightarrow\psi^{-1}$ and $U(\psi)\rightarrow(4\psi^2)^{-1}$ to yield two linearly independent solutions:

$$H_m(\psi)\underset{\psi\rightarrow\infty}{\longrightarrow} C_m^{+}\psi^{(n_m^{+}-1/2)}+C_m^{-}\psi^{(n_m^{-}-1/2)}, \tag{9}$$

where $n_m^{\pm}=(1\pm m)/2$. From Eq. (3) it can be seen that the far field solutions must match to the asymptotic value of the electric potential $\Phi\rightarrow(yV_{CT}B_\infty)/c$ for large r. Since y can be expressed in polar coordinates as $y\equiv r\sin\theta\sin\phi$, it can be written as $y=(2/B_\infty)^{1/2}\psi^{1/2}\sin\phi$ for large ψ. After comparing this with Eqs. (7) and (9), we see that only the $m=1$ solutions are acceptable, viz., $C_m^{+}=0$ for $m\neq1$. The solution that decays as $\psi\rightarrow\infty$ is also unacceptable because it connects to the corresponding near-field solution which blows up as $\psi\rightarrow0$.

Hence the electric potential in frame f' has the form $\Phi(\psi,\phi)=H_1(\psi)\sin\phi$. In frame f' the plasma flows are perceived to be caused by the drift motion in f', $\mathbf{v}'=(\mathbf{E}'\times\mathbf{B}_0')c/B_0'^2$. Note that on the spherical CT boundary the flows are purely azimuthal. At infinity they approach the expected uniform behavior $v'\rightarrow-V_{CT}\hat{\mathbf{x}}$. In the rest frame f the plasma flow is given by $\mathbf{v}=\mathbf{v}'+\mathbf{V}_{CT}$ which is also consistent with the frozen flow condition for low-frequency disturbances, $\mathbf{E}+\mathbf{v}\times\mathbf{B}_0/c=0$. By this method, the electric field E in f can be determined near the CT and since it is localized and of the form $\mathbf{E}=\mathbf{E}(x-V_{CT}t,y,z)$, it is seen to be in contact with successive flux tubes for a period $\sim r_1/V_{CT}$. A pulse of this duration excites Alfvén waves having a characteristic frequency $\omega\sim2\pi V_{CT}/r_1$. Near the surface of the CT the magnitude of E is roughly $E\sim E_y\sim V_{CT}B_\infty/c$. It therefore serves as a boundary condition for the electric fields of the Alfvén wave which radiate outward along the magnetic field lines with velocity V_{A0}. The parallel wavelength of the disturbance is therefore $\lambda_\parallel\sim(V_{A0}/V_{CT})r_1$. Typically $\lambda_\parallel$ is 1 to 2 m which is considerably smaller than the tokamak connection length $\sim2\pi qR$ which for ETR is tens of meters. Hence the outgoing Alfvén power is effectively radiated to infinity. Since the oscillatory magnetic field of the Alvén wave is $b_x\sim(ck_\parallel/\omega)E_y$, the total Alvén wave power radiated away is approximately $P_\omega=2\pi r_1^2cE_yb_x/4\pi$ or

$$P_\omega=\tfrac{1}{2}r_1^2B_\infty^2V_{CT}^2/V_{A0}. \tag{10}$$

It is worthwhile mentioning that the result (10) is a factor of $\frac{9}{16}$ smaller than a calculation of Barnett and Olbert,[10] who considered the drag on a moving spherical conducting body across a magnetized plasma. However, their approach was different because they assumed that the sphere *did not* displace or deform the external magnetic field as is the case here. An effective wave drag force acting on the CT is given by $\mathbf{F}_\omega=-(P_\omega/V_{CT}^2)\mathbf{V}_{CT}$.

An additional drag mechanism comes from the $1/R$ ($R=$ major radius) toroidal field gradient,[6] which causes a drag force on a spherical body given by $\mathbf{F}_{\nabla B}\simeq\frac{1}{2}(B^2/R)r_1^3\hat{\mathbf{x}}_R$, where $\hat{\mathbf{x}}_R$ is a unit vector pointing in the major radius direction.

Accordingly, the equation of motion of the CT is

$$\frac{d\mathbf{V}_{CT}}{dt}=-\frac{\mathbf{V}_{CT}}{\tau_\omega}+\frac{V_{A1}\hat{\mathbf{x}}_R}{\tau_{\nabla B}}, \tag{11}$$

where $\tau_\omega=\frac{2}{3}\tau_{A1}(n_1/n_0)^{1/2}$ and $\tau_{\nabla B}=\frac{2}{3}R/V_{A1}$ are the two characteristic slowing down times. The initial velocity, V_{CT0}, is determined by the requirement that the final velocity be zero at the desired fuel deposition point. Taking this to be the magnetic axis of the tokamak having minor radius a, and assuming $\tau_{\nabla B}$, τ_ω, and V_{A1} remain unchanged along a trajectory parallel to $-\hat{\mathbf{x}}_R$ we obtain a transcendental equation for V_{CT0}:

$$a=V_{CT0}\tau_\omega-\frac{V_{A1}\tau_\omega^2}{\tau_{\nabla B}}\ln\left[1+\frac{V_{CT0}}{V_{A1}}\frac{\tau_{\nabla B}}{\tau_\omega}\right]. \tag{12}$$

The penetration time is given by

$$t_p=\tau_\omega\ln\left[1+\frac{V_{CT0}}{V_{A1}}\frac{\tau_{\nabla B}}{\tau_\omega}\right]. \tag{13}$$

Taking previous ETR parameters with $a=0.834$ m, $R=3$ m, and $n_0=10^{14}$ cm^{-3} gives $\tau_\omega=19$ μs, $\tau_{\nabla B}=13$ μs, $V_{CT0}=171$ km/s, $V_{inj}=230$ km/s, and $t_p=10.7$ μs. After coming to rest, the CT will be accelerated and expelled from the plasma by the ∇B force after a "dwell time" $\tau_D=(2\tau_{\nabla B}a/V_{A1})^{1/2}\sim11$ μs. Therefore the ideal fueling scenario requires proper timing: Disassembly and fuel release should begin after a penetration time, and the duration of disassembly should be much less than the dwell time.

Next, we discuss two possible disassembly mechanisms. First, the CT magnetic field is annihilated by dissipative magnetic merging processes occurring at the thin field reversal layer on the surface of the CT. It follows that the fluid in this layer is subjected to a pressure of $B^2/8\pi$, and is squeezed out with velocity V_{A1} along the layer, and ejected at the location of the poles into the external plasma as fresh fuel. This process leads to a shrinkage and decay of the CT. To understand and esti-

mate this process heuristically, we apply a modified version of the early reconnection or current sheet magnetic field annihilation models of Sweet[11] and Parker.[12] In the steady phase of magnetic merging the layer thickens to a value $\delta=\eta/\mu_0 v_1$ by striking a balance between magnetic flux diffusion and convection: v_1 being the surface collapse velocity and η the resistivity. Equating the mass flow rate into the layer $4\pi r_f^2\rho_1 v_1$ to the outflow rate, $-2\pi(\delta)^2 V_{A1}$ gives another expression, $v_1=2\delta^2 V_{A1}/r_f^2$. Combining the two expressions for v_1 gives $\delta=(r_f^2\eta/\mu_0 2V_{A1})^{1/3}$. Using this expression for δ gives the contraction rate of the CT boundary surface

$$v_1\equiv dr_1/dt=2^{1/3}\eta^{2/3}V_{A1}^{1/3}/\mu_0^{2/3}r_f^{2/3}, \tag{14}$$

and from integrating a CT lifetime

$$t_{\text{lifetime}}=0.48\mu_0^{2/3}r_1^{5/3}/\eta^{2/3}V_{A1}^{1/3}. \tag{15}$$

Using the same parameters and using classical Spitzer resistivity with $T\approx 2$ eV [see below Eq. (6)] we get $t_{\text{lifetime}}=13.6$ μs, which is fortunately comparable to the penetration time ~ 11 μs.

Since the magnetic topology in this problem contains no magnetic X-type neutral lines, the generally accepted steady reconnection models of Petschek and others,[13] which predict rapid reconnection rates of the order of $v_1\sim 0.1V_{A1}$ or more in the neighborhood of neutral lines, may not be relevant. Fast reconnection remains an active and controversial area. It is worth mentioning that the current sheet model of Sweet-Parker reconnection does not explain the rapid reconnection rates observed in astrophysical phenomena. However, their model can be restored if one replaces the classical resistivity with an anomalous hyperresistivity produced by tearing mode turbulence.[14] For CT parameters, hyperresistivity and classical resistivity are comparable for turbulence levels of $\tilde{B}/B\sim 0.1$, so that shorter CT lifetimes could be expected.

The second disassembly mechanism involves a cyclic process: resistive decay of the internal CT magnetic field followed by its recompression by the external magnetic field pressure. During an incremental internal δt the square of the CT magnetic field decays by the amount $\delta B^2=-(2\mu^2\eta/\mu_0)B^2\delta t$. Imagine that after the interval δt the field is instantaneously recompressed up to its original value to maintain equilibrium. By flux conservation $\delta(Br_f^2)=0$, so the incremental change in the radius is $\delta r_1=r_1\delta B^2/4B^2$. We thus conclude that the radius shrinks at the rate

$$dr_1/dt=-10\eta/\mu_0 r_1. \tag{16}$$

At these high CT densities the impurity radiative cooling rate ($\sim n_f^2$) is quite large and leads to a low steady-state plasmoid temperature, typically around 5 eV or less, giving a characteristic collapse time of ~ 20 μs. During collapse, density and therefore β increases until a critical β is reached. Presumably this causes the CT to break up and deposit its fuel.

In conclusion, the model here explores what we believe to be the three essential physics issues facing the problem of fueling a tokamak by ejection of compact toroids. The model is predicated on the assumption that the closed magnetic fuel topology of the CT is held together by the external tokamak magnetic field, excluded from its interior, thereby forming a stable equilibrium. Questions of stability of the current sheet, Rayleigh-Taylor instability during slowing down, and a complete solution of Eq. (8) for the motionally induced electric field potential are left for future study.

I am indebted to J. M. Greene, R. F. Bourque, and W. M. Nevins for helpful discussions.

[1]D. P. Schissel *et al.*, Nucl. Fusion **27**, 1063 (1987).

[2]R. J. Fonck *et al.*, in Proceedings of the Sixth International Conference on Plasma Surface Interactions in Controlled Fusion Devices, Nagoya, Japan, May 1984 [J. Nucl. Mater. **128**, 330 (1984)].

[3]M. Greenwald *et al.*, Phys. Rev. Lett. **53**, 352 (1984).

[4]B. Coppi, contribution to the Annual Controlled Fusion Theory Conference, Lake Tahoe, Nevada, 1984 (unpublished), invited paper No. 3A3.

[5]J. H. Hammer, C. W. Hartman, and J. L. Eddeman, in Proceedings of the Eighth Symposium on the Physics and Technology of Compact Toroids, University of Maryland, College Park, Maryland, June 1987 (to be published).

[6]L. J. Perkins, S. K. Ho, and J. Hammer, Lawrence Livermore National Laboratory Report No. UCRL 96894 (to be published).

[7]M. N. Rosenbluth and M. N. Bussac, Nucl. Fusion **19**, 489 (1979).

[8]S. Jardin, Nucl. Fusion **22**, 629 (1982).

[9]D. E. Shumaker, A. A. Mirin, and J. H. Hammer, contribution to the Sherwood Theory Conference, 18–20 April 1988, Gatlinburg, Tennessee (unpublished), paper No. 3C25.

[10]A. Barnett and S. Olbert, J. Geophys. Res. **91**, 10117 (1986).

[11]P. A. Sweet, Nuovo Cimento Suppl. **8**, Ser. X, 1988 (1958).

[12]E. N. Parker, Astrophys. J. Suppl. Ser. **8**, 177 (1963).

[13]V. M. Vasyliunas, Rev. Geophys. Space Phys. **13**, 303 (1975).

[14]H. R. Strauss, Astrophys. J. **326**, 412 (1988).

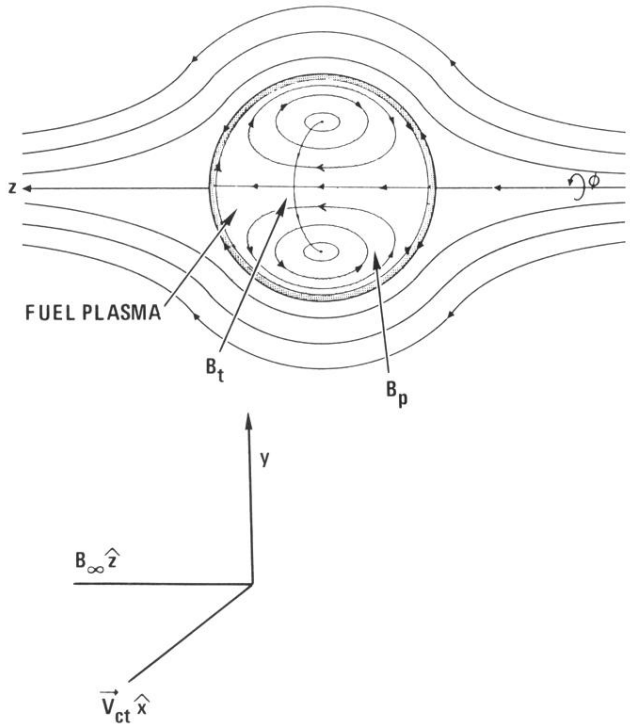

FIG. 1. Magnetic field topology in the vicinity of a compact spheromak moving in $+\hat{\mathbf{x}}$ direction. A spheroid current sheet (shaded circle) separates oppositely directed magnetic field lines.